An Acad Bras Cienc (2022) 94(Suppl. 1): e20210810 DOI 10.1590/0001-3765202220210810
Anais da Academia Brasileira de Ciências | *Annals of the Brazilian Academy of Sciences*
Printed ISSN 0001-3765 I Online ISSN 1678-2690
www.scielo.br/aabc | www.fb.com/aabcjournal

GEOSCIENCES

The 1991 explosive Hudson volcanic eruption as a geochronological marker for the Northern Antarctic Peninsula

HEITOR EVANGELISTA, ALEXANDRE CASTAGNA, ALEXANDRE CORREIA, MARIUSZ POTOCKI, FRANCISCO AQUINO, ALEXANDRE ALENCAR, PAUL MAYEWSKI, ANDREI KURBATOV, RICARDO JAÑA, JULIANA NOGUEIRA, MARCUS LICINIO, ELAINE ALVES & JEFFERSON C. SIMÕES

Abstract: It is estimated that the explosive Hudson volcano eruption in Southern Chile injected approximately 2.7 km^3 of basalt and trachyandesite tephra into the troposphere between August 8-15, 1991. The Hudson signal has been detected in Antarctica at the eastern sector and in South Pole snow. In this work, we track the Hudson volcanic plume using a dispersion model, remote sensing, and a re-analysis of a high-resolution ice core analysis from the Detroit Plateau in the Antarctic Peninsula and sedimentary records from shallow lakes from King George Island (KGI). The Hudson eruption imprint in these records is confirmed by using a weekly resolved aerosol concentration database from KGI demonstrating that the regional impact of Hudson eruption predominates over the Mount Pinatubo/Phillippines volcanic signal, dated from June 1991, in terms of particulate matter depositions. The aerosol elemental composition of Ca, Fe, Ti, Si, Al, Zn, and Pb increases from 2 to 3 orders of magnitude in background level during the days following the eruption of the Hudson volcano.

Key words: Aerosols, Antarctic Peninsula, Hudson volcano, Volcanism.

INTRODUCTION

The early years of the 1990 decade in Antarctica were characterized by important volcanic ash deposition over the continental ice sheets. Past volcanic activity can be recorded in ice cores as visible volcanic ash (tephra) layers and/or sulfate-rich layers, which have the potential to indicate large-scale atmospheric load (Cole-Dai & Mosley-Thompson 1999). Tephra layer analysis in ice cores can be useful for establishing ice core chronology, reconstructing past atmospheric circulation patterns, and investigating long-term links between volcanic aerosols and climatic change (Zhou et al. 2006).

The second-largest volcanic eruption of the 20th century occurred at Mount Pinatubo in the Philippines on June 12-15, 1991. The first detection of Pinatubo aerosols in Antarctica comes from McMurdo and South Pole Station reports in late 1991 (Cacciani et al. 1993, Deshler et al. 1994). Stratospheric horizontal winds played a significant controlling factor in the long-range aerosol dispersion of Pinatubo eruption products (Cole-Dai et al. 1999). However, no less relevant was the Hudson volcano (southern Chile) contribution during August 8-9, August 12-15, and September 9-15, 1991, due to the explosive character of its eruptions and its closest proximity to Antarctica.

The active stratovolcano Hudson is the southernmost volcano in the Chilean Andes. Contrary to Pinatubo ash dispersion, Hudson volcano injected more pyroclastic material into the troposphere with subsequent and rapid deposition (Inbar et al. 1995, Kilian et al. 1993, Legrand & Wagenbach 1999). It is estimated that during the 1991 explosive eruptions of Hudson volcano, approximately 2.7 km^3 of basalt and trachyandesite tephra were ejected to a maximum height of 12 km above sea level (ASL) (Kratzmann et al. 2010). Most of the volcanic material had drifted southwards, reaching the Southern Ocean and the Antarctic continent. In contrast, Pinatubo sulfur-rich clouds reached 25-35 km containing around 1.8 million tons of SO_2 (Krueger et al. 1995), whose impact was spread out all around the globe. In a South Pole snowpit, measurement of sulfate concentration in snow layers dated 1991-1992 distinguished between the Hudson and the Pinatubo deposit (Cole-Dai et al. 1997a, 1999, Palmer et al. 2001). The Hudson peak was observed at that site during December 1991, while Pinatubo peaked in December 1992 and all along 1993.

By the time 1991 Hudson eruptions started, Pinatubo ash had already spread nearly worldwide, with a fine fraction starting to disperse poleward by late August/early September (Trepte et al. 1993). Examination of Pinatubo material dispersion, using the Total Ozone Mapping Spectrometer (TOMS) satellite sensor covering the period between August 13 and September 30, suggests that its impact around the Antarctic Peninsula was not as pronounced as in around the tropics and sub-tropics (Figure 1). The region encompassing Southern Patagonia, south of latitude 45°S, and

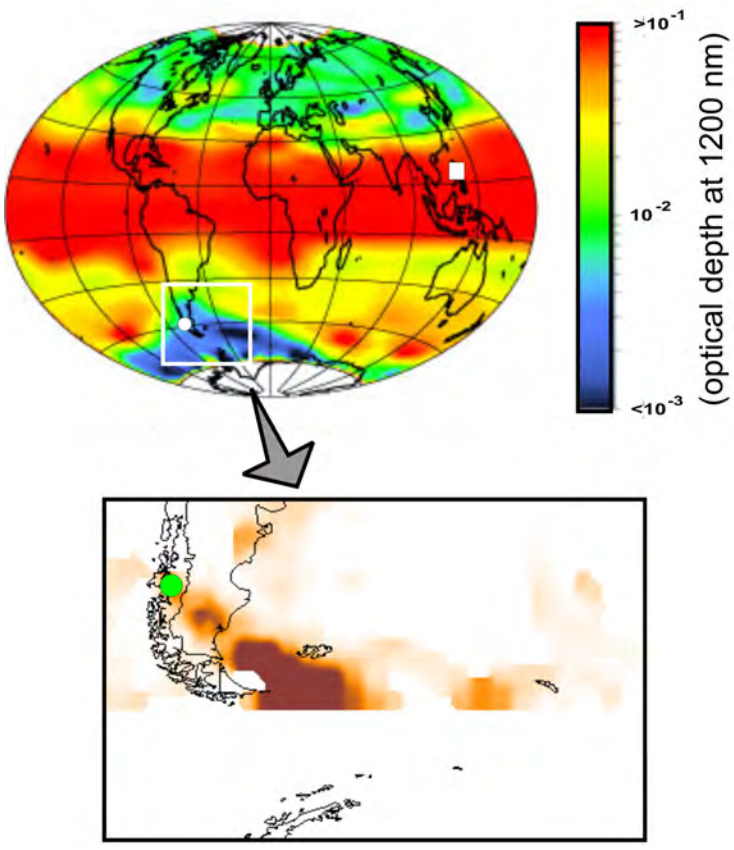

Figure 1. Image in the upper part was acquired by the Stratospheric Aerosol and Gas Experiment II (SAGE II) flying aboard NASA's Earth Radiation Budget Satellite (ERBS). It corresponds to the dispersion of Pinatubo (white square) ash around the globe (1020 nm Optical Depth). It shows composite data between August 13 to September 30 of 1991 (https://earthobservatory.nasa.gov/images/1510/global-effects-of-mount-pinatubo). In the window below, the sector where Hudson (green dot) ash had the most significant impact on August 12 of the same year (inferred from the aerosol index product TOMS/NASA sensor).

the Southern Ocean – approximately between the longitudes 30° W and 120° W – was also less impacted. Although this period partially covers the Hudson eruption, no impact of the Hudson eruption was observed in the NASA SAGE II measurement of aerosol optical depth since it refers to the stratospheric dispersion of the Pinatubo signal.

A Dispersion model applied to the Hudson eruption using the Lagrangian ash tracking model PUFF proposed by Kratzmann et al. (2010) reproduced the aerial distribution extent and temporal evolution of the 1991 volcanic plume with prevailing ash and aerosol loads within the troposphere. Their model projected the presence of Hudson volcanic materials over the South Atlantic and the Southern Ocean. Another important and more obvious factor is the proximity between the southern Andean region and Antarctica compared to Mount Pinatubo/Philippines and the action of the westerly winds that blow Patagonian mineral particles (dust and volcanic ash) towards the Southern Ocean (Erickson et al. 2003, Gassó et al. 2010, Gassó & Stein 2007).

To better elucidate the impact of the 1991 volcanic events, we reanalyzed a weekly resolved aerosol elemental concentration database from King George Island/Admiralty Bay, obtained in the context of the Brazilian Antarctic Program; an elemental concentration database developed from a high-resolution ice core retrieved in the Northern Antarctic Peninsula/Detroit Plateau, obtained in the context of the US-Brazil-Chile project CASA (Climate of Antarctica and South America); and three shallow sediment cores in King George Island/Admiralty Bay that include the year 1991. We combined these databases with the modeling of volcanic ash dispersion to track the influence of Hudson volcanic eruptions.

MATERIALS AND METHODS

Study site databases

This work was conducted in two sites on the Northern Antarctica Peninsula: (1) King George Island/Admiralty Bay in the South Shetland Islands, and (2) Detroit Plateau in the Antarctic Peninsula, Figure 2. The Antarctic Peninsula is a relatively narrow mountain ridge that extends over 520,000 km^2 from the base of West Antarctica (Marie Byrd Land) at latitude 74°S towards its Northern limit in the Drake Passage (Figure 2a). The Bellingshausen Sea bounds the peninsula on the west side while the Weddell Sea lies east.

At the tip of the Antarctic Peninsula is located the South Shetland Islands in the northern portion of the Bellingshausen Sea (Figure 2a). The climatic regime of the South Shetland Islands is defined as maritime subpolar (Simonov 1977). It is highly influenced by the migration of subpolar cyclones that bring to this region warm air, high nebulosity, and humidity from the South Pacific, resulting in precipitation as rain and snow (Bintanja 1995). King George Island is located between the Drake Passage and the Bransfield Strait between coordinates 61°50'S – 62°15'S and 57°30'W – 59°00'W. It comprises an area of 1,140 km^2 with 30 km width, a maximum extension of 79 km at the SW-NE direction, and a maximum altitude around 700 m a.s.l. (Figure 2a). The Antarctic Peninsula is the northernmost part of the Antarctic continent and is 80% ice-covered with an ice sheet of approximately 500 m thick (Bindschadler 2006). It has a sharp elevation gradient, with most glaciers flowing into the Weddell Sea at its Eastern Sector, which has been experiencing significant breakup since 2002 (Turner et al. 2009). These mountains form a significant barrier to the persistent westerly winds that transport moisture and warmer air masses to its location. In view of this physiography, the

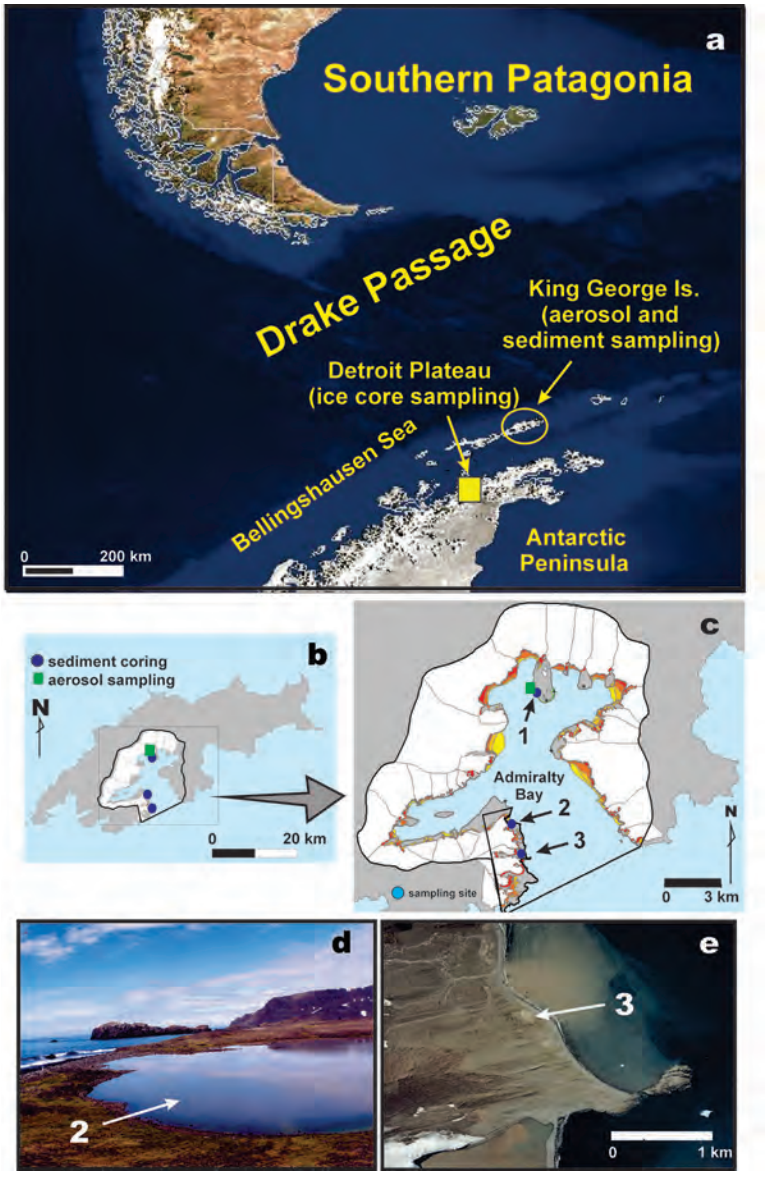

Figure 2. (a) General location of the study site indicating ice core and sediment core sampling and aerosol monitoring; (b) King George Island with Admiralty Bay (with glaciers drainage system) highlighted; (c) location of sampling sites (1/2/3) inside Admiralty Bay; (d) sediment coring site: terminus of Ecology glacier; (d) sediment coring site: Agatha Point.

regional climatic regime differs significantly at each side of the Antarctic Peninsula. During the austral summer, snow and ice cover more than 90% of its total surface area. Additionally, air mass advections from South America influence the South Shetland Islands since cyclonic migration through this region increases the meridional wind component southwards. This mechanism is responsible for the atmospheric transport of terrigenous particles and biotic material from South America (Hebel et al. 2018, Pereira et al. 2004).

Detroit Plateau (64°10'S; 60°0'W) is a major interior plateau of Graham Land, located in the northern sector of the Antarctic Peninsula, with a mean elevation of ~1900 m.a.s.l.. Local mean annual accumulation is on average 2.5 m w.e. for the last 27 years (Potocki et al. 2016), allowing sufficient resolution to study events on a seasonal basis. Air mass advections from South America influence Detroit Plateau to some extent, albeit less so than for the South Shetland Islands.

Satellite products and dispersion model

The dispersion of the volcanic ash plumes was simulated daily by using the Hybrid Single-Particle Lagrangian Integrated Trajectory – HYSPLIT/NOAA (Stein et al. 2015). HYSPLIT is a dispersion model that uses a hybrid Lagrangian model approach and Eulerian methodology. In the particle model case for volcanic ash dispersion, a fixed number of particles are advected about the model domain by the mean wind field and spread using a turbulent component. The model's default configuration assumes a 3-dimensional particle distribution. The model can be driven by several meteorological databases, and in this case, we used the NCEP/NCAR Reanalysis (Kalnay et al. 1996). HYSPLIT calculates the dispersion and deposition of volcanic material extending from the volcano summit to a user-specified maximum height. The model considers the terrain geomorphology and runs for spherical particles of density 2.5 10^6 g m^{-3} with diameters ranging from 0.3 to 30 ≒m. Simulations were carried out for the August and September eruptions, with a maximum height as specified by reports of the height of the ash column. For the first set of simulations, each emission day was followed independently for consecutive 48 hours. A second simulation presents a cumulative view over ten days.

In addition to the dispersion model, we use the Aerosol Index (AI), from the TOMS sensor, onboard the Nimbus-7 (11/1978 to 4/1993) satellite. The AI is calculated based on the difference between the observed and the simulated backscattered ultraviolet (UV) radiation for an atmosphere without aerosols (Herman et al. 1997). The simulation also considers the surface UV reflectivity by using the climatology established over clear atmosphere observations. This method enables the detection of absorbing aerosols (smoke, dust, ash) over water, land, and snow/ice (Hsu et al. 1999a). The index is unitless, and its magnitude depends not only on aerosol optical properties and concentration but also on its altitude and therefore is used mostly in a qualitative way (e.g., Ginoux & Torres 2003, Hsu et al. 1999b), but relative use is also possible when considering short periods or short spatial scales. Here we use the TOMS AI data Version 8. All positive AI values indicate the presence of absorbing aerosols, but smaller values can represent the effects of uncertainty on the assumptions used in the simulation for an aerosol-free atmosphere, and we use only values greater than 0.7. The original data can be found on the Total Ozone Mapping Spectrometer website https://ozoneaq.gsfc.nasa.gov/data/toms/#.

Aerosol sampling and elemental composition analysis

Aerosols were collected at the Laboratory of Atmospheric Science located 2 km away from the Brazilian Antarctic Station Comandante Ferraz (62°05'07"S 58°23'29"W). Samples were collected using a double filtration system of Nuclepore polycarbonate filters of 0.4 mm (fine aerosol mode) and 8.0 mm (course aerosol mode) porosity. Data presented here refers to the total elemental composition (fine+course fractions). Air filtration was carried out 24 hours per day and integrated for one week in 1991. A 47 mm-diameter aerosol filter holder was placed in an inlet outside the laboratory at approximately 10 m a.s.l.. The pumping system (a Single-head GAST pump system) operated with rates between 10 to 16 L min^{-1}. The inlet has a microparticle cutoff size of 10 mm. Filters containing aerosols were analyzed using the PIXE (Particle-Induced X-Ray Emission) technique at the Institute of Physics at the São Paulo University (USP), Brazil. This technique is based on detecting characteristic X-rays emitted by elements in the sample target, as they are bombarded by high energy fluxes

of proton particles of 2.4 MeV generated by a compact isochrone cyclotron (CGR-MeV). The detection limit for PIXE reaches 10^{-7}g $g^{-1,}$ and the range of element detectability varies from Na to U. Characteristic X-rays are measured by a Kevex Si(Li) detector.

Ice core sampling and elemental composition analysis

An ice core was retrieved from Detroit Plateau (64°05'07" S; 059°38'42" W; 1,937 m a.s.l.) in the Antarctic Peninsula in December 2007, within the US-Brazil-Chile joint research program CASA (Climate of the Antarctic and Southern America; https://www.polartropical.org/casa/). The Detroit Plateau ice cap temperature during coring activities was approximate -14°C. The ice core was transported frozen from Antarctica to CCI - Climate Change Institute/Maine University, United States of America.

An electromechanical system provided by the University of Maine drilled to 120 m depth through snow, firn, and ice. The Ice core was 9 cm in diameter and was cut *in situ* into segments varying from 85 to 95 cm. Density values were obtained at the campsite. The upper 98 m of this core was processed using ultra-clean handling procedures. Ice core sampling was conducted inside a cold room (-20°C) at CCI, where the ice core sections were cut into 10cm long samples, and the surface layer (~ 2 cm) was removed by an acid-washed Teflon knife. Ice samples for trace-element analysis were collected directly into acid-cleaned (10% trace metal grade HNO3) polypropylene Nalgene jars. Before analysis, each sample was acidified to 1% with Optima double-distilled HNO3 under a class- 100 HEPA clean bench and left to digest for 60 days (Potocki et al. 2016). Then, at the Climate Change Institute (University of Maine), the samples were analyzed with an Inductively Coupled Plasma Mass Spectrometer (ICP-MS) for elemental composition. The dating of the ice core was based on H_2O_2 measurements that yielded a clear interannual sinusoidal variability (Potocki et al. 2016).

Shallow lake sediment coring, chronology, and elemental analysis

Periglacial shallow lakes selected for the present work are located at Admiralty Bay/King George Island. The choice of these lakes is related to the observed increase in susceptibility of the region to regional variability associated with dramatic ice mass losses (Sancho et al. 2017, Skvarca et al. 1998). These lakes receive direct atmospheric depositions and water melting from winter/spring fresh snow. Admiralty Bay is characterized by a high density of glacial drainage basins (nearly 32 according to Dani et al. 2012 and Bremer et al. 2004). Two of the three shallow lakes used in this work are located near the bay's mouth (1. near the terminus of Ecology glacier: coordinate 62°10'39" S, 058°27'61" W with 17 cm long; and 2. at Agatha Point: coord. 62°10'8" S, 058°26'8" W with 16 cm long), the other sampling site is located in the inner part of the Bay at "Ipanema": coord. 62°05'12" S, 058°25'1" W with 26 cm long). All sediment cores were sampled manually to avoid disturbances. We used acrylic tubes with an inner diameter of 7 cm and a wall thickness of 3 mm. During the field campaign, sediment layers varying from 0.5 to 1 cm were subsampled from the cores for radiometric dating and chemical analysis.

Sediment dating was performed using an extended range CANBERRA gamma spectrometry system with a 25 % relative efficiency co-axial GeHp detector. The gamma detection system is encased in 10 to 15 cm of low background lead shielding and internally coated with 1 mm copper sheets. The instrumentation is currently installed in the Laboratory of Radioecology and Global Changes (LARAMG) of the Rio de Janeiro

State University/Brazil. The gamma system provides a peak resolution of 1.8 keV at 1.33 MeV and 0.850 keV at 122 keV. The calibration standard to construct the detector efficiency curve, as a function of the gamma energy, was a liquid cocktail of radionuclides (^{133}Ba, ^{57}Co, ^{139}Ce, ^{85}Sr, ^{137}Cs, ^{54}Mn, ^{88}Y, and ^{65}Zn) in 0.5 M of HCl. The standard was manufactured by the AEA Technology with a total activity concentration of 132 kBq and a volume of 100.76 g. Each sediment layer was dried for 24 hours at 50°C. After that, fine sediment samples (around 20 g) were placed in cylindrical plastic pots sealed and submitted to the counting of gamma-ray photons for 86400 seconds each. Radionuclides of dating interest were ^{210}Pb, ^{226}Ra, and ^{137}Cs (Appleby & Oldfield 1992). To interpret ^{210}Pb data in the sediment cores, the mathematical model was used known as Constant Rate of Supply (CRS). It assumes variations in sedimentation rates of a sediment core that cannot be explained by bioturbation phenomena or a physical mixture of sediments (Appleby & Oldfield 1992). This model is based on two premises: ^{210}Pb Excess is supplied to the surface of the sediment at a constant rate; b) The radioactive ^{210}Pb decay is constant due to its small post-depositional mobility. The ^{210}Pb present in the rocks comes from ^{238}U radioactive disintegration chain. At the time ^{226}Ra disintegrates and forms ^{222}Rn, a noble gas, part of it emanates from the rocks into the atmosphere, where it undergoes further disintegration up to ^{210}Pb. As this radionuclide is solid, it precipitates in the surface by gravity or "washout" and joins with ^{210}Pb formed in the crystalline structure of the sediment grains of the original rock. This deposited ^{210}Pb is called excess or without support to distinguish it from the ^{210}Pb derivative *in situ* of the ^{226}Ra decay (supported).

For chemical analysis, aliquots from each stratum were taken and dried at 40°C for 24 hours. Metal extraction was made by leaching the samples with 4 mL of HNO_3 at 0.5 M, and 1 mL of HCl at 0.5 M in 3 runs at 150°C. The extraction product was obtained in a sequential step by adding 1 mL of 0.5 M HCl and 25 ML of Milli-Q water to complete a final volume. All reagents used were Suprapur Merk$^{\dot{O}}$. Blanks underwent the same procedure and were measured with the samples to assess possible contamination. The quantification of metals occurred employing an Optical Emission Spectrometry with Inductively Coupled Plasma (ICP-OES Ultima II, from Jobin-Yvon). This multi-elementary technique uses an inductive plasma source (from the ionization of argon gas) to atomize and ionize the products of the chemical extraction. The ICP-OES measures the electromagnetic radiation emitted by the atoms or ions excited by the plasma.

In this work, the quantitative method was used. To increase sensitivity, an ultrasonic nebulizer was used to reduce the size of the particles that form the aerosol to be taken to the plasma flame. The applied power was 1000 Watts.

RESULTS AND DISCUSSIONS

Volcanic material depositions characterized the first years of the 1990 decade in Antarctica as a result of the Pinatubo and Hudson volcanic eruptions (Cole-Dai et al. 1999, Kilian et al. 1993, Legrand & Wagenbach 1999).

In our simulations of the dispersion of Hudson volcanic material originated at the eruptive episode on August 12-15, 1991, Figure 3, the plumes migrated in a general SE direction, thus directly impacting the South Shetland Islands (especially on August 13-14) and the adjacent Southern Ocean.

The Hudson 1991 eruption reached a Volcanoes Explosivity Index (VEI) of 5 (Global Volcanism Program, Smithsonian Institution,

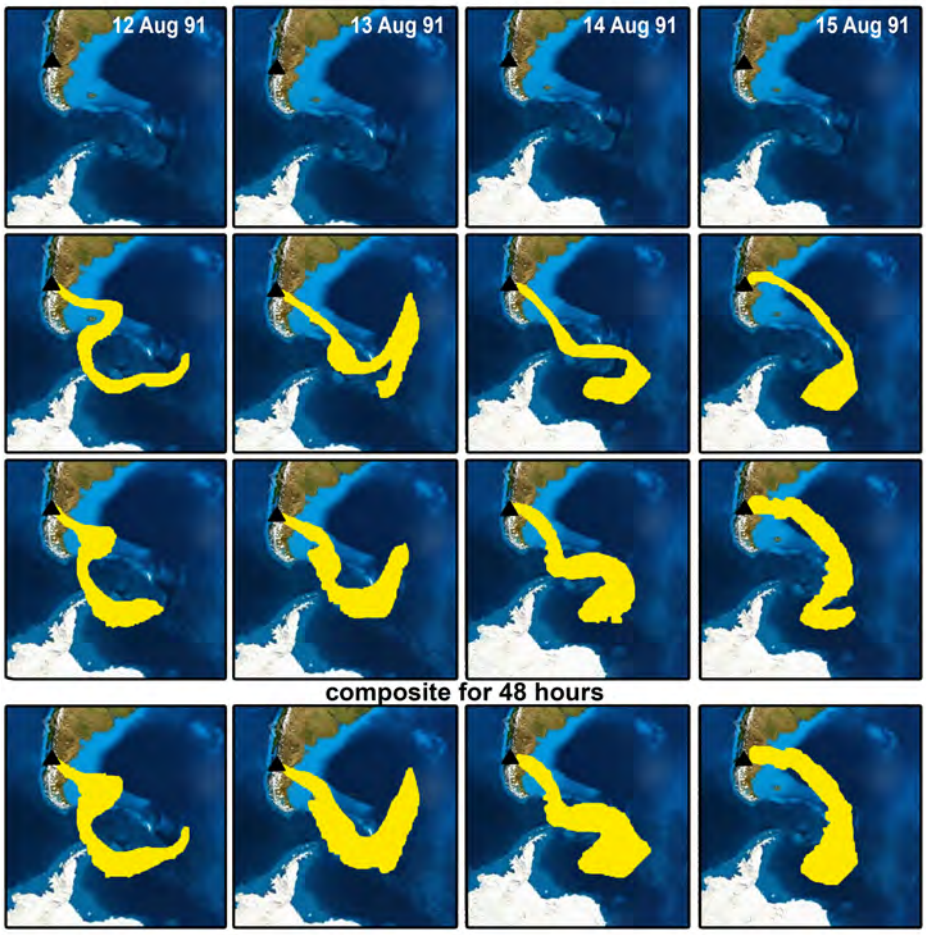

Figure 3. Transport and dispersion of volcanic ash simulated by the HYSPLIT/ NOAA Volcanic Ash Model (https://www.ready.noaa.gov/HYSPLIT_ash.php) originated from the Hudson volcano (black triangle) during the second eruptive episode on August 12-15 and subsequent days.

https://volcano.si.edu/), indicating an injection of a bulk tephra volume of more than 1 km³ into the troposphere and stratosphere. The eruptive event ejected about 2.7 km3 (dense-rock equivalent) of basalt and trachyandesite magma as tephra fell (Scasso & Carey, 2005). Hudson volcanic aerosols were transported poleward, mainly in the troposphere and lower stratosphere beneath the polar vortex directed by the westerlies (Legrand & Wagenbach 1999).

A combined analysis of the Aerosol Index and the transport and dispersion simulation for the volcanic eruption in the subsequent days of August 12-15, 1991 (Figure 4) illustrates the general dynamics of the plume around the Antarctic continent. It can be observed that a high load of volcanic material was deposited closer to the northern tip of the Antarctic Peninsula. In the Weddell Sea sector, an existing cyclonic system sped up the surface winds in clockwise movement impacting the Antarctic Peninsula from August 19 to August 23, 1991. In approximately one month, the plume from Hudson circled Antarctica, and due to prevailing winds (westerlies), most of the ash was deposited in the Southern Ocean. Similar effects of dilution and deposition hampering remote sensing observations from source to sampling site were described for dust emissions from Patagonia (Gassó et al. 2010). Chemical analysis of the Hudson volcano eruptive products revealed a composition of 58-63% of silica (SiO_2), medium- to high-K_2O content, relative enrichment of TiO_2, Na_2O, and enrichment in LIL (Large Ion Lithophile; i.e., K, Rb, Cs, Sr, Ba, and Pb), HFSE (High Field Strength Elements; i.e., Ti, Zr, Hf, Nb, and Ta),

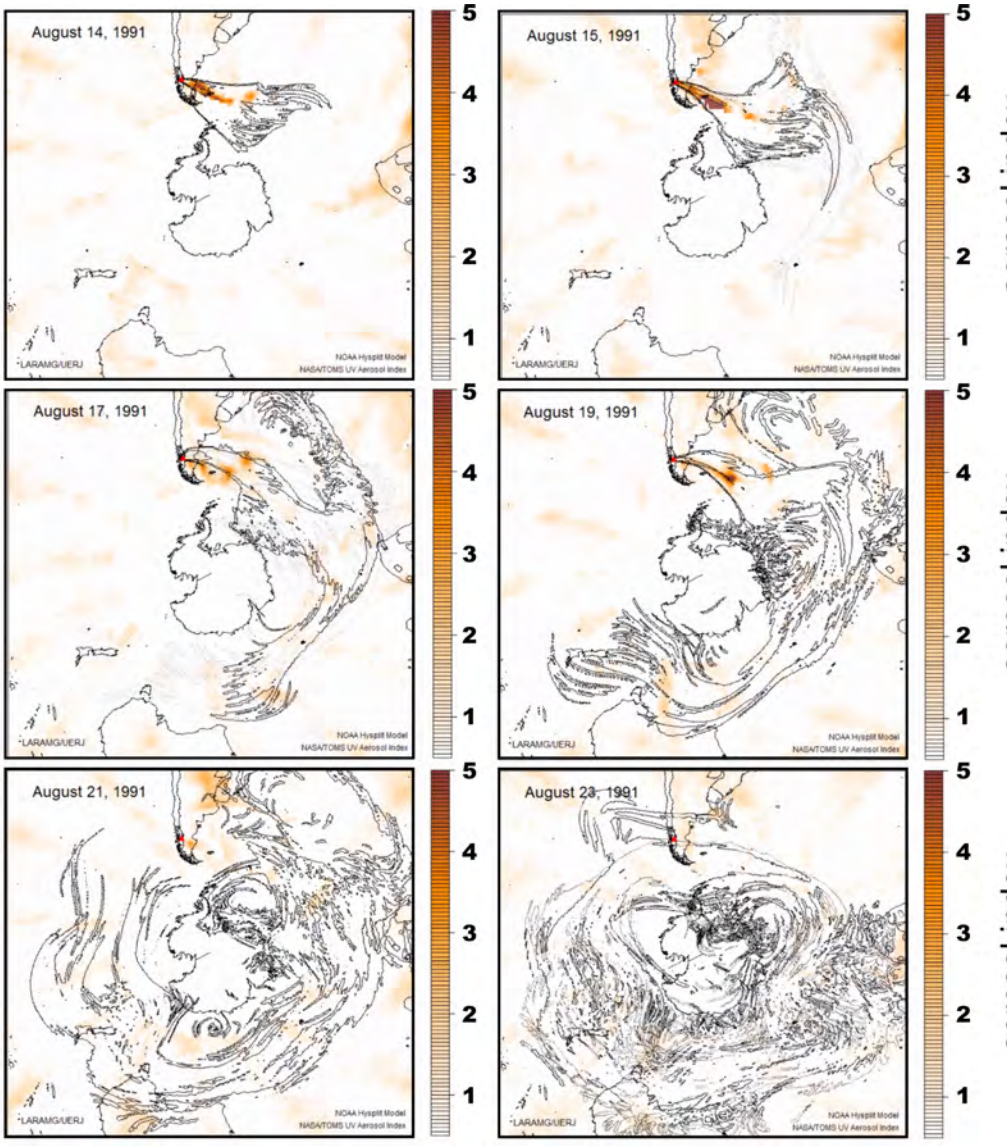

Figure 4. Joint analysis of the Aerosol Index and the transport and dispersion of volcanic ash simulations originated at Hudson volcano (red dot) from the second eruptive episode and subsequent days. The envelope of the dispersion plume is shown.

and REE (Rare Earth Elements) (Inbar et al. 1995, Scasso & Carey 2005). Chemical analysis of the aerosol samples collected at the King George Island (Figure 5a), weekly resolution, reveals high enrichment in Ca, Fe, Ti, Si, and Al during the volcanic activity of Hudson, more notably after the 12-15 August event. Although with lower resolution (seasonal), concentrations of Fe, Ti, Si, and Ba are found to be highly elevated in the August 1991 snow layer in the Detroit Plateau ice core (Figure 5b). Concentrations of Pb and Zn in the sediment for this period are much higher than the baseline value (Figure 6).

The increase from 2 to 3 orders of magnitude over background for the days following the eruption in Southern Chile is noted in both aerosols and the ice core from the Antarctic Peninsula, suggesting a major contribution of the Hudson eruption. The combination of continuous aerosol monitoring before, during, and after the volcanic episode together with the dispersion model and Aerosol Index data constitute a definitive demonstration that the anomalous increases observed in the atmosphere, ice core, and in sediments of the pro-glacial environment of the Northern Antarctic Peninsula are related

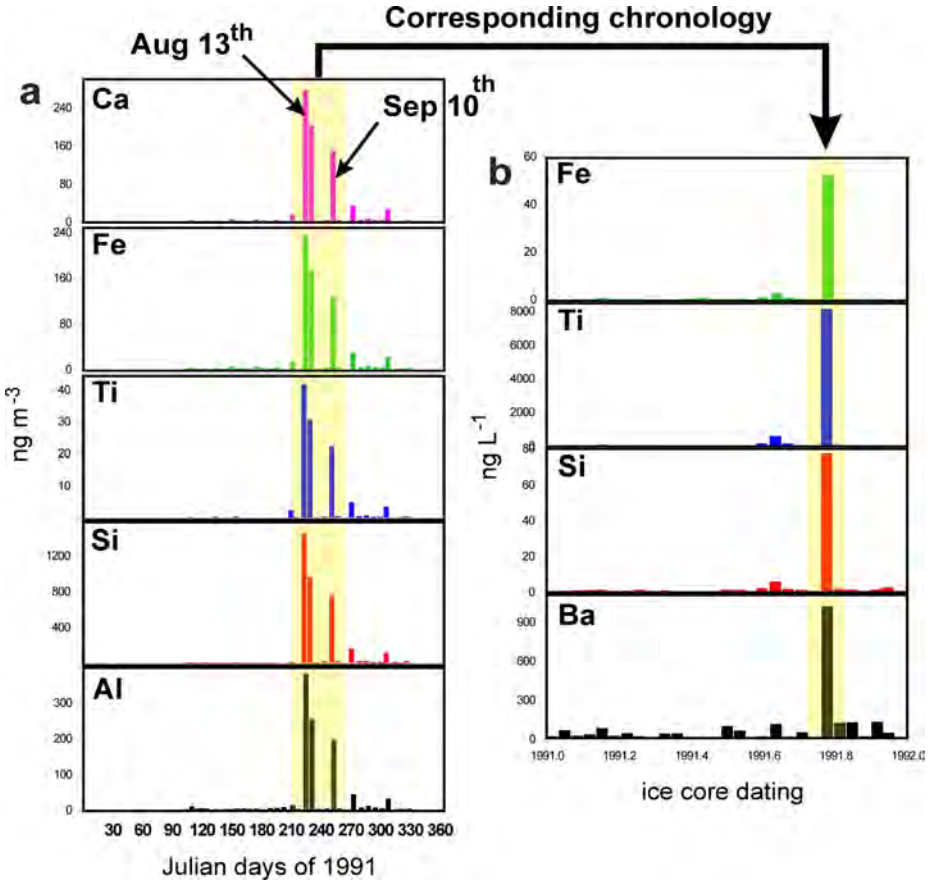

Figure 5. (a) Aerosol elemental composition monitored in King George Island in 1991 depicting increases in Ca, Fe, Ti, Si, and Al, when compared to the annual background, coincident with the eruption activity of Hudson volcano; (b) Ice core chronology, based on H_2O_2 data from Potocki et al., 2016, at Detroit Plateau Antarctic Peninsula showing a corresponding increase in Fe, Ti, Si, and Ba.

to the 1991 Hudson eruptive episode. Due to the recognized global-scale impact of Mount Pinatubo volcanism on the climate system, many researchers have attributed the changes in this part of the Southern Ocean, especially at the Northern Antarctic Peninsula, in 1991 exclusively to the Pinatubo eruption. Verona et al. (2019) have suggested that Pinatubo induced cooling in the Southern Ocean and warming up to 0.8 °C off the Antarctic Peninsula. This happens for two reasons: (a) models in use do not assimilate most of the moderate-intensity volcanisms (Gao et al. 2008); (b) the real impact extension of Hudson volcanic event is not fully described for higher latitudes. Our results may shed some light on the significant impact of Hudson particulate matter precipitation at the Northern Antarctic Peninsula, despite our work not wanting to establish any direct relationship with the climate issue.

Another interesting aspect observed in this work is the interpretation of the abrupt increases in metal composition, like Al, Fe, Ti, and Ca, in the ice core. Such events are usually attributed to dust storm advection, but our observations show that explosive eruptions can substantially elevate concentrations of the elements.

Volcanic signal detection is observed in other locations around Antarctica, suggesting a widespread impact on the continent. Ice cores retrieved close to the Amundsen-Scott South Pole Station have significant deposition of SO_4^{-2}, related to the Hudson eruption event in September 1991 (Cole-Dai et al. 1997b). Similarly, the DT263 ice core, retrieved from an East Antarctic location, exhibited SO_4^{-2} concentrations dated to 1991 and was identified as a Hudson

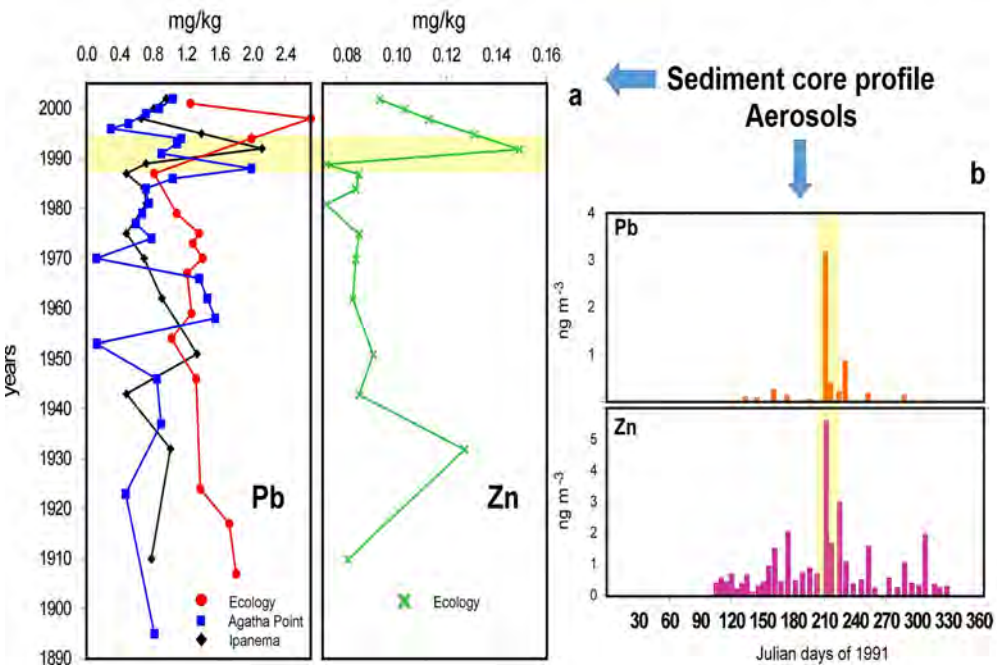

Figure 6. (a) Sedimentary profile of Pb and Zn in pro-glacial lakes of King George Island/Admiralty Bay; (b) Pb and Zn concentrations in aerosols of King George Island/ Admiralty Bay. The peak corresponding to Hudson volcanic eruption is highlighted.

volcano contribution (Zhou et al. 2006). Although the Hudson volcanic eruption produced less SO_2, when compared to Pinatubo's production (~ 8%), the volcanic aerosol mass from the former extended southward immediately and reached the Antarctica continent more effectively (Zhou et al. 2006). Also, the Hudson plume was lower in altitude than Pinatubo's; this resulted in the deposition of Hudson ash almost immediately following the eruption, while the Pinatubo materials reached the atmosphere over Antarctica later in the year and deposited following that of the Hudson materials. The stratospheric SO_2 clouds dispersion resulting from the Hudson eruption was tracked by TOMS for many days and identified in East Antarctica by 20th August 1991 (Carn et al. 2003, Constantine et al. 2000).

Figure 7 summarizes the identified Hudson eruptions impacts around the whole Antarctic continent, depicting the widespread distribution of the volcanic aerosols due to the westerlies and a comparable result concerning the Aerosol Index data and transport/dispersion of volcanic material simulations presented here (Figure 4).

CONCLUSIONS

We tracked the Hudson volcanic plume using the HYSPLIT particle mode and the Aerosol Index data for the eruption episode between August and mid-September 1991. Remote sensing data indicates a rapid dispersion of the eruption plume from the Hudson volcano to the Antarctic Peninsula, with a more expressive impact from the second event, between 12-15 August 1991. Our simultaneous weekly resolved aerosol sampling from King George Island captured that event based on an anomalous increase in elemental Ca, Fe, Ti, Si, and Al, relative to the background in the days following the eruption, and compatible with the Hudson tephra chemical composition. The impact was also recorded in a simultaneous increase in Fe, Ti, Si, and Ba concentrations in an ice core from Detroit Plateau on the Antarctic Peninsula and in high Pb and Zn concentrations in shallow sediment cores retrieved on King George Island at the same time. Although our work has surveyed only the elemental compositions (not volcanic glass shards or cryptotephra), the above pieces

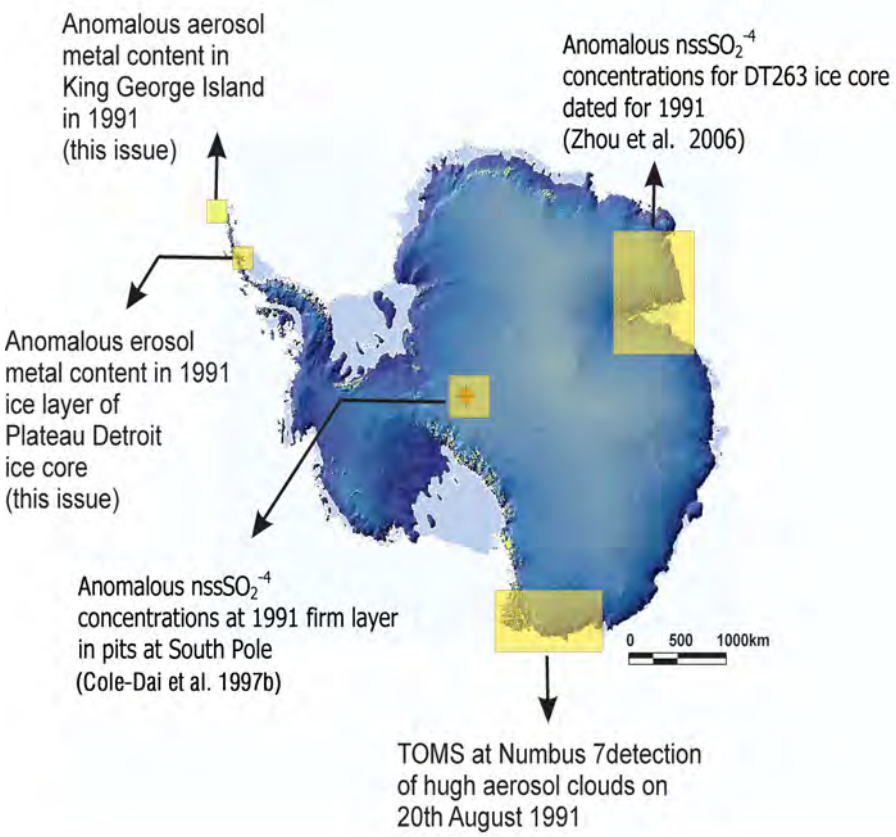

Figure 7. A composite from the current literature of sites where 1991 Hudson volcanism was detected (including data in this issue).

of evidence strongly suggest an association with the volcanic event.

Although the 1991 Pinatubo eruption had a greater global impact, its most distant location concerning Antarctica and the characteristic of its explosion led to the muted deposition of the eruption materials in the Antarctic ice sheet. Therefore, the 1991 Hudson eruptive event is of greater significance as a geochronological signal for the Northern Antarctic Peninsula. This work highlights Southern Andean volcanism as a key player in the West Antarctic and the Antarctic Peninsula climate, with immediate and direct impacts over the continent. Abrupt increases in metal composition in the ice cores, usually attributed to dust storm advection, can be observed following important eruptive events.

Acknowledgments

This research was funded by the Conselho Nacional de Desenvolvimento Científico e Tecnológico (CNPq), projects 550041/2007-9 and 573720/2008-8 – INCT Criosfera. The authors are grateful for the participation of colleagues Luiz Fernando M. Reis and Marcelo Arevalo in the fieldwork. We thank Robert Priori for the figure's layout and the Brazilian Antarctic Program, Chilean Air Force (FACh), and the Chilean Antarctic Institute for logistics in Antarctica. The authors would like to thank the revisors for the important suggestions.

REFERENCES

APPLEBY PG & OLDFIELD F. 1992. Application of lead-210 to sedimentation studies. In: IVANOVICH M & HARMON RS (Eds), Uranium Series Desiquilibrium: Application to Earth, Marine and Environmental Science, Oxford, United Kingdom: Clarendon Press, p. 731-783.

BINDSCHADLER R. 2006. The environment and evolution of the West Antarctic ice sheet: setting the stage. Phil Trans R Soc A 364: 1583-1605.

BINTANJA R. 1995. The local surface energy balance of the Ecology Glacier, King George Island, Antarctica: measurements and modelling. Antarct Sci 7(3): 315-325.

BREMER UF, ARIGONY-NETO J & SIMÕES JC. 2004. Teledetecção de mudanças nas bacias de drenagem da Ilha Rei George, Ilhas Shetlands do Sul, Antártica, entre 1956 e 2000. Pesquisa Antártica Brasileira 4: 37-48.

CACCIANI M, DI GIROLAMO P, DI SARRA A, FIOCCO G & FUÀ D. 1993. Volcanic aerosol layers observed by lidar at South Pole, September 1991-June 1992. Geophys Res Lett 20(9): 807-810.

CARN SA, KRUEGER AJ, BLUTH GJS, SCHAEFER SJ, KROTKOV NA, WATSON IM & DATTA S. 2003. Volcanic eruption detection by the Total Ozone Mapping Spectrometer (TOMS) instruments: A 22-year record of sulphur dioxide and ash emissions. Geol Soc Spec Publ 213: 177-202.

COLE-DAI J & MOSLEY-THOMPSON E. 1999. The Pinatubo eruption in South Pole snow and its potential value to ice-core paleovolcanic records. Ann Glaciol 29: 99-105.

COLE-DAI J, MOSLEY-THOMPSON E & QIN D. 1999. Evidence of the 1991 Pinatubo volcanic eruption in South Polar snow. Chinese Sci Bull 44(8): 756-760. COLE-DAI J, MOSLEY-THOMPSON E & THOMPSON LG. 1997a. Annually resolved southern hemisphere volcanic history from two Antarctic ice cores. J Geophys Res-Atmos 102(14): 16761-16771.

COLE-DAI J, MOSLEY-THOMPSON E & THOMPSON LG. 1997b. Quantifying the Pinatubo volcanic signal in south polar snow. Geophys Res Lett 24(21): 2679-2682.

CONSTANTINE EK, BLUTH GJS & ROSE WI. 2000. TOMS and AVHRR observations of drifting volcanic clouds from the august 1991 eruptions of Cerro Hudson. Geoph Monog Series 116: 45-64.

DANI N, ARIGONY-NETO J, SIMÕES JC, VELHO LF, RIBEIRO RR, PARNOW I, BREMER UF, FONSECA JUNIOR ES & ERWES HJ. 2012. A new topographic map for Keller Peninsula, King George Island, Antarctica. Pesquisa Antártica Brasileira 5: 105-113.

DESHLER T, JOHNSON BJ & ROZIER WR. 1994. Changes in the Character of Polar Stratospheric Clouds Over Antarctica in 1992 Due to the Pinatubo Volcanic Aerosol. Geophys Res Lett 21(4): 273-276.

ERICKSON DJ, HERNANDEZ JL, GINOUX P, GREGG WW, MCCLAIN C & CHRISTIAN J. 2003. Atmospheric iron delivery and surface ocean biological activity in the Southern Ocean and Patagonian region. Geophys Res Lett 30(12): 1-4.

GAO C, ROBOCK A & AMMANN C. 2008. Volcanic forcing of climate over the past 1500 years: An improved ice core-based index for climate models. J Geophys Res 113(D23): D23111.

GASSÓ S & STEIN AF. 2007. Does dust from Patagonia reach the sub-Antarctic Atlantic Ocean? Geophys Res Lett 34(1): 3-7.

GASSÓ S, STEIN A, MARINO F, CASTELLANO E, UDISTI R & CERATTO J. 2010. A combined observational and modeling approach to study modern dust transport from the Patagonia desert to East Antarctica. Atmos Chem Phys 10(17): 8287-8303.

GINOUX P & TORRES O. 2003. Empirical TOMS index for dust aerosol: Applications to model validation and source characterization. J Geophys Res [Atmos] 108(D17): 4534.

HEBEL I, DACASA RÜDINGER MC, JAÑA RA & BASTIAS J. 2018. Genetic Structure and Gene Flow of Moss Sanionia uncinata (Hedw.) Loeske in Maritime Antarctica and Southern-Patagonia. Front Ecol Evol 6: 152.

HERMAN JR, BHARTIA PK, TORRES O, HSU C, SEFTOR C & CELARIER E. 1997. Global distribution of UV-absorbing aerosols from Nimbus 7/TOMS data. J Geophys Res-Atmos 102(D14): 16911-16922.

HSU NC, HERMAN JR, GLEASON JF, TORRES O & SEFTOR CJ. 1999a. Satellite detection of smoke aerosols over a snow/ice surface by TOMS. Geophys Res Lett 26(8): 1165-1168.

HSU NC, HERMAN JR, TORRES O, HOLBEN BN, TANRE D, ECK TF, SMIRNOV A, CHATENET B & LAVENU F. 1999b. Comparisons of the TOMS aerosol index with Sun-photometer aerosol optical thickness: Results and applications. J Geophys Res [Atmos] 104(D6): 6269-6279.

INBAR M, OSTERA HA, PARICA CA, REMESAL MB & SALANI FM. 1995. Environmental assessment of 1991 Hudson volcano eruption ashfall effects on southern Patagonia region, Argentina. Environ Geol 25(2): 119-125.

KALNAY E ET AL. 1996. The NCEP/NCAR 40-Year Reanalysis Project. B Am Meteorol Soc 77: 437-472.

KILIAN R, IPPACH P & LÓPEZ-ESCOBAR L. 1993. Geology, Geochemistry and recent activity of the Hudson Volcano, Southern Chile. In: ISAG, 2., Oxford. Proceedings..., Oxford, p. 385-388.

KRATZMANN DJ, CAREY SN, FERO J, SCASSO RA & NARANJO J-A. 2010. Simulations of tephra dispersal from the 1991 explosive eruptions of Hudson volcano, Chile. J Volcanol Geotherm Res 190(3-4): 337-352.

KRUEGER AJ, WALTER LS, BHARTIA PK, SCHNETZLER CC, KROTKOV NA, SPROD I & BLUTH GJS. 1995. Volcanic sulfur dioxide measurements from the total ozone mapping spectrometer instruments. J Geophys Res 100(D7): 14057.

LEGRAND M & WAGENBACH D. 1999. Impact of the Cerro Hudson and Pinatubo volcanic eruptions on the Antarctic air and snow chemistry. J Geophys Res-Atmos 104(D1): 1581-1596.

PALMER AS, VAN OMMEN TD, CURRAN MAJ, MORGAN V, SOUNEY JM & MAYEWSKI PA. 2001. High-precision dating of volcanic events (A.D. 1301-1995) using ice cores from Law Dome, Antarctica. J Geophys Res-Atmos 106(D22): 28089-28095.

PEREIRA KCD, EVANGELISTA H, PEREIRA EB, SIMÕES JC, JOHNSON E & MELO LR. 2004. Transport of crustal microparticles from Chilean Patagonia to the Antarctic Peninsula by SEM-EDS analysis. Tellus B 56(3): 262-275.

POTOCKI M, MAYEWSKI PA, KURBATOV AV, SIMÕES JC, DIXON DA, GOODWIN I, CARLETON AM, HANDLEY MJ, JAÑA R & KOROTKIKH EV. 2016. Recent increase in Antarctic Peninsula ice core uranium concentrations. Atmos Environ 140: 381-385.

SANCHO LG, PINTADO A, NAVARRO F, RAMOS M, DE PABLO MA, BLANQUER JM, RAGGIO J, VALLADARES F & GREEN TGA. 2017. Recent Warming and Cooling in the Antarctic Peninsula Region has Rapid and Large Effects on Lichen Vegetation. Sci Rep-UK 7(1): 5689.

SCASSO RA & CAREY S. 2005. Morphology and formation of glassy volcanic ash from the August 12-15, 1991 eruption of Hudson volcano, Chile. Lat Am J Sedimentol Basin Anal 12(1): 3-21.

SIMONOV IM. 1977. Physical-geographic description of the fildes peninsula (South Shetland Islands). Polar Geog 1(3): 223-242.

SKVARCA P, RACK W, ROTT H & IBARZÁBAL Y DONÁNGELO T. 1998. Evidence of recent climatic warming on the eastern Antarctic Peninsula. Ann Glaciol 27: 628-632.

STEIN AF, DRAXLER RR, ROLPH GD, STUNDER BJB, COHEN MD & NGAN F. 2015. NOAA's HYSPLIT Atmospheric Transport and Dispersion Modeling System. B Am Meteorol Soc 96(12): 2059-2077.

TREPTE CR, VEIGA RE & MCCORMICK MP. 1993. The poleward dispersal of Mount Pinatubo volcanic aerosol. J Geophys Res-Atmos 98(D10): 18563-18573.

TURNER J, BINDSCHADLER R, CONVEY P, DI PRISCO G, FAHRBACH E, GUTT J, HODGSON DA, MAYEWSKI PA & SUMMERHAYES CP. 2009. Antarctic Climate Change and the Environment, Cambridge: Scientific Committee on Antarctic Research, 555 p.

VERONA LS, WAINER I & STEVENSON S. 2019. Volcanically Triggered Ocean Warming Near the Antarctic Peninsula. Sci Rep 9(1): 9462.

ZHOU L, LI Y, JIHONG C-D, TAN D, SUN B, REN J, WEI L & WANG H. 2006. A 780-year record of explosive volcanism from DT263 ice core in east Antarctica. Chinese Sci Bull 51(22): 2771-2780.

How to cite

EVANGELISTA H ET AL. 2022. The 1991 explosive Hudson volcanic eruption as a geochronological marker for the Northern Antarctic Peninsula. An Acad Bras Cienc 94: e20210810. DOI 10.1590/0001-3765202220210810.

Manuscript received on May 28, 2021;
accepted for publication on January 21, 2022

HEITOR EVANGELISTA[1]
https://orcid.org/0000-0001-9832-1141

ALEXANDRE CASTAGNA[2]
https://orcid.org/0000-0002-6069-1574

ALEXANDRE CORREIA[3]
https://orcid.org/0000-0003-0044-9097

MARIUSZ POTOCKI[4,5]
https://orcid.org/0000-0002-1110-9568

FRANCISCO AQUINO[6]
https://orcid.org/0000-0003-2993-1100

ALEXANDRE ALENCAR[1]
https://orcid.org/0000-0002-8104-1781

PAUL MAYEWSKI[4]
https://orcid.org/0000-0002-3360-763X

ANDREI KURBATOV[4,6]
https://orcid.org/0000-0002-9819-9251

RICARDO JAÑA[7]
https://orcid.org/0000-0003-3319-1168

JULIANA NOGUEIRA[1,8]
https://orcid.org/0000-0003-4858-8774

MARCUS LICINIO[9]
https://orcid.org/0000-0003-3589-5652

ELAINE ALVES[1]
https://orcid.org/0000-0001-9620-9498

JEFFERSON C. SIMÕES[4,6]
https://orcid.org/0000-0001-5555-3401

[1]Universidade do Estado do Rio de Janeiro, Departamento de Biofísica e Biometria, LARAMG – Laboratório de Radioecologia e Mudanças Climáticas, Rua São Francisco Xavier, 524, 20550-013 Rio de Janeiro, RJ, Brazil

[2]Protistology and Aquatic Ecology, Ghent University, Krijgslaan 281, 9000, Gent, Belgium

[3]Universidade de São Paulo, Instituto de Física, Departamento de Física Aplicada, Rua do Matão, 1371, 05508-090 São Paulo, SP, Brazil

[4]Climate Change Institute, University of Maine, 168 College Avenue, 04469, Orono, Maine, USA

[5]School of Earth and Climate Sciences, University of Maine, 168 College Avenue, 04469, Orono, Maine, USA

[6]Universidade Federal do Rio Grande do Sul, Centro Polar e Climático, Instituto de Geociências, Av. Bento Gonçalves, 9500, 90650-001 Porto Alegre, RS, Brazil

[7]Chilean Antarctic Institute, Plaza Benjamín Muñoz Gamero 1055, Punta Arenas, Magallanes, Chile

[8]Faculty of Forestry and Wood Sciences, Czech University of Life Sciences Prague, Kamýcká 129, 165 00, Prague, Czech Republic

[9]Universidade Federal do Espírito Santo/UFES, CCS, Departamento de Ciências Fisiológicas, Laboratório de Radiometria Ambiental, Prédio Basico I, Av. Marechal Campos, 1468, 29043-900 Vitória, ES, Brazil

Correspondence to: **Juliana Nogueira**
E-mail: de_sousa_nogueira@fld.czu.cz

Author contributions

Evangelista, H.: paper writing and coordination of related activities in the paper. Castagna A.: remote sensing analysis. Correia, A.: aerosol sampling in King George Island and elemental analysis. Potocki, M.: logistics, ice core sampling at Detroit Plateau and ice core dating. Simões, J.C.: paper writing and discussions/ ice core sampling at Detroit Plateau. Aquino, F.: logistics and ice core sampling at Detroit Plateau. Alencar, A.S.: aerosol sampling and ice core drilling at Detroit Plateau. Mayewski, P.A. : Ice core analysis and discussions. Kurbatov, A.: ice core drilling at Detroit Plateau paper discussions. Jaña, R.: logistics and ice core sampling at Detroit Plateau. Nogueira, J.: paper writing and discussions. Marcus V.V.J. Licinio: Sediment coring at King George Island, dating and elemental composition. Alves, E.: Atmospheric dispersion modeling.